MVA2015 IAPR International Conference on Machine Vision Applications, May 18-22, 2015, Tokyo, JAPAN

Color Image Processing from the Physical, Psychological, and Biological Viewpoints

Johji Tajima
Nagoya City University
tajima@nsc.nagoya-cu.ac.jp

Abstract

Color image processing is necessary in various academic fields, but each field approaches it differently, and often incorrectly. It should really be done in a way that is meaningful from the physical, psychological, or biological point of view. In this paper, I introduce the database SOCS, which is a tool to combine the physical and psychological viewpoints, and two recent researches, one on the illumination estimation relating to the physical viewpoint, and the other on the genetic polymorphism relating to the biological viewpoint.

1. Introduction

'Color image' has been processed from a variety of viewpoints. The meaning of 'color image processing' changes from one researcher to another. As color images are used mainly for object recognition in machine vision research, color is mainly dealt with from the physical viewpoint, in which a color image is simply a multi-channel image that can be processed as a set of three grayscale images. There, it is not so important that the color processed corresponds to the color perceived by a human being. This approach, including the multi-spectral image analysis, can be called the 'color image processing from the physical viewpoint.'

However, 'color' is a sense that is proper to mankind. Though there are many animals that recognize color, the color seen by a fish, for example, is not the same as the color seen by mankind. As color influences human emotion and preference, there are industrial fields where the color sensed by human beings is regarded important. In the industries of photography, graphic arts, and illumination, accurate color reproduction is required. In the cosmetics industry, color appearance under various illuminations is important.

For accurate color reproduction, it may be necessary to understand the physiological processing of color by the human nervous system including the brain. However, because it is not yet fully understood, the processing by nerves and the brain is studied by psychological or psychophysical methods. In human vision, three kinds of cones have their proper spectral sensitivities. Thus, in an artificial system that concerns human color perception, it is necessary that the color sensors have spectral sensitivities whose linear combinations conform to the sensitivities of the cones (the Luther condition). The difference in color is perceived as the result of a complicated processing of the cone outputs by the nervous system. To simulate this, color difference is normally evaluated by the distance in the L*a*b* or L*u*v* uniform color space defined by the CIE, or their improvements. These color spaces have been determined by psychophysical experiments. Color image processing for color reproduction is executed on this basis, and its result is subjectively evaluated. Such an approach is the color image processing from the psychological viewpoint. This kind of approach is also required in machine vision when the purpose of the system is related to human perception, such as when it is necessary to visually recognize the traffic signs or signals in the same manner as a human being does.

Researches from these two viewpoints have long been done separately; however, more interdisciplinary researches should be conducted to yield more fruitful technologies.

In addition to the above two, the third 'biological' viewpoint has become important. Conventional color image processing has been aimed at 'normal' trichromat vision. However, 'barrier-free' or 'universal' design has become more important in everyday life. Certain genetic variety exists in the population that causes dichromatic or anomalous trichromatic color perception. There also exists a genetic polymorphism within those with 'normal' trichromatic vision. To better accommodate such various human color perception, color image processing algorithms simulating dichromats or anomalous trichromats are being developed. However, there are few researches on the color appearance for each genetic type.

Recently, we obtained a very interesting result on the relationship between genetic polymorphism and subjective color difference. Color image processing technology can contribute to both the analysis of human color vision and the development of solutions for the genetically caused problems. This may be called the color image processing from the biological viewpoint.

In this paper, we discuss our research and development efforts from these viewpoints.

2. Color sensor evaluation and SOCS

Let us first define the spectral vector space. For simplicity, let us define the visible light wavelength to be from 380nm to 780nm and discretize it with 5nm interval. Then, the light spectral intensity is expressed by an 81-dimensional vector **S**. In the same way, human cone

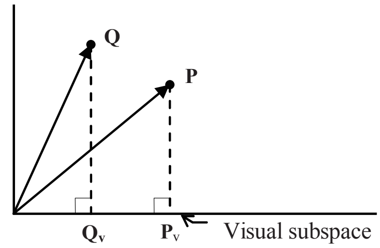

Fig.1 Visual perception of light.

spectral sensitivities $\bar{\mathbf{l}}, \bar{\mathbf{m}}, \bar{\mathbf{s}}$ are expressed by 81-dimensional vectors. The color stimuli, which are sensed by the human retina, are expressed by L, M, S as Eq.(1).

$$L = \mathbf{S} \cdot \bar{\mathbf{l}}, M = \mathbf{S} \cdot \bar{\mathbf{m}}, S = \mathbf{S} \cdot \bar{\mathbf{s}} \tag{1}$$

This relationship is depicted in Fig.1. In this figure, the 81-dimensional spectral space is simplified to two dimensions, and the (human) visual three-dimensional subspace (visual subspace), which is spanned by $\bar{\mathbf{l}}, \bar{\mathbf{m}}, \bar{\mathbf{s}}$ in the 81-dimensional space, is represented by one horizontal dimension. Then, the light stimuli **P** and **Q** are shown by two vectors and the color stimuli are obtained as vectors $\mathbf{P_v}$ and $\mathbf{Q_v}$, which are orthographic projections to the visual subspace.

Color images are usually input by the sensors with red, green and blue filters, which establish three sensitivities to light signal. To be able to obtain an accurate color reproduction, these three sensitivities are required to satisfy the 'Luther condition', which says that each of the sensitivities must be a linear combination of the human cone sensitivities. This means that, in the vector space, the subspace spanned by the sensor sensitivity vectors (sensor subspace) should coincide with the visual subspace. The Luther condition can be expressed by Eq.(2), where the sensor spectral sensitivities are $\bar{\mathbf{r}}, \bar{\mathbf{g}}, \bar{\mathbf{b}}$.

$$\begin{pmatrix} \bar{\mathbf{r}}^t \\ \bar{\mathbf{g}}^t \\ \bar{\mathbf{b}}^t \end{pmatrix} = \begin{pmatrix} c_{11} & c_{12} & c_{13} \\ c_{21} & c_{22} & c_{23} \\ c_{31} & c_{32} & c_{33} \end{pmatrix} \cdot \begin{pmatrix} \bar{\mathbf{l}}^t \\ \bar{\mathbf{m}}^t \\ \bar{\mathbf{s}}^t \end{pmatrix} \tag{2}$$

If the sensors satisfy this condition, any pair of light stimuli that look as different colors with eyes can be discriminated using the sensor outputs. This can be mathematically proved [1]. As such, the Neugebauer quality factor q_e, which directly measures the degree to which the Luther condition is satisfied, has been known as an index for sensor evaluation [2].

However, q_e is not necessarily a good measure for the sensor evaluation, for we know that color images look sufficiently natural if we linearly compensate the input signals, R, G and B, as Eq.(3), even when we use a set of easily selected red, green, and blue filters whose q_e is low.

$$\begin{pmatrix} R' \\ G' \\ B' \end{pmatrix} = \begin{pmatrix} a_{11} & a_{12} & a_{13} \\ a_{21} & a_{22} & a_{23} \\ a_{31} & a_{32} & a_{33} \end{pmatrix} \cdot \begin{pmatrix} R \\ G \\ B \end{pmatrix} \tag{3}$$

In such a case, the sensor subspace does not coincide with the visual subspace (Fig.2). The lights **P** and **Q** are perceived by the human vision as the orthographic projection $\mathbf{P_v}$ and $\mathbf{Q_v}$ to the visual subspace, and the color signals obtained by the sensors are the orthographic projections $\mathbf{P_s}$ and $\mathbf{Q_s}$ to the sensor subspace. Because the Luther condition is not satisfied, the colors are metamerically matched differently. In spite of the fact, the reproduced image looks sufficiently natural. The reason is deemed to be as follows.

Colors we see are mostly those of reflective objects. If the spectral intensity of the reflected light is widely distributed as shown in Fig.3(a), for example, the lights $\mathbf{P}_1$ and $\mathbf{P}_2$, which look like the same color $\mathbf{P_v}$ to the human vision, would appear in different colors $\mathbf{P}_{1s}$ and $\mathbf{P}_{2s}$ to the sensors. However, if the spectral intensity is distributed thinly in the dimensions higher than the dominant three dimensions (Fig.3(b)), and if its distribution is known, we can reconstruct the original $\mathbf{P}_1$ and $\mathbf{P}_2$ from $\mathbf{P}_{1s}$ and $\mathbf{P}_{2s}$ by assuming they are on the principal axes inferred from the distribution. Re-projecting the reconstructed vectors to the visual subspace, the approximate color $\mathbf{P'_v}$ can be obtained. This reconstruction and re-projection procedure can be ex-

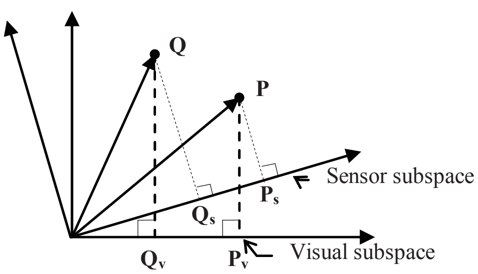

Fig.2 Visual subspace and sensor subspace.

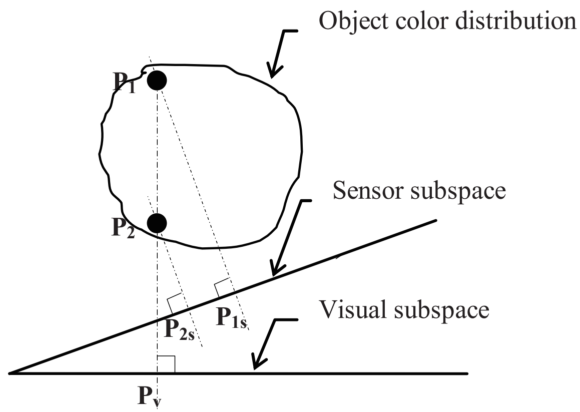

(a) Color appearance of wide color distribution.

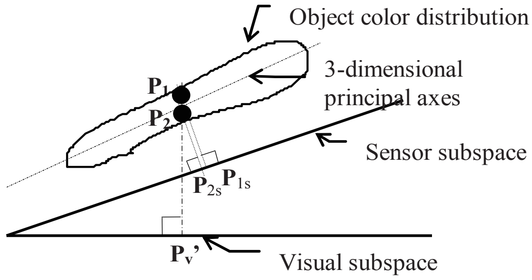

(b) Color appearance of thin color distribution.

Fig.3 Relation between color reproduction and object color distribution.

pressed by the matrix compensation in Eq.(3).

In such a scenario, the quality of the color reproduction also depends on the shape of the object color distribution. Accordingly, it is necessary to know the distribution of objects' spectral reflectance in order to evaluate the quality of the color compensation. For that purpose, we collected spectral reflectance/transmittance data that cover almost all that are usually observed. Table 1 shows the number of the collected spectral data.

Though the Pointer gamut [3], which measured the color of many objects under the daylight, had been known, it was expressed by the tristimulus values, and thus the colors under other illuminations could not be reproduced. From the new spectral data, we could obtain accurate color appearance under any illumination variation. The data were published as **ISO/TR 16066 "Standard object colour spectra database for colour reproduction evaluation (SOCS)"** in 2003, whose development was reported in [4]. This technical report (TR) was published as one of graphic technology standards, and is known in the color reproduction industry, but may not be well known in other areas. SOCS is very useful in many application areas such as color sensor evaluation, color gamut evaluation, illumination light source evaluation, and accurate color reproduction.

Many computer vision papers still deal with color in a very primitive manner. We hope more researchers become more serious about spectral distribution and develop a new usage of SOCS.

Based on SOCS, some research results have been derived as follows:

- Since the spectral transmittance of color slides and the spectral reflectance of lithographic prints, which constitute the most of print material, can be sufficiently approximated by three principal components, the conventional scanners, whose source images are mostly from those, do not need to satisfy the Luther condition [5]. Figure 4 shows the spectral reflectance/transmittance rms (%) errors between the original spectra and those approximated by the corresponding number of principal components.
- Spectral reflectance restoration quality after the linear compensation is closely related to the subspace dimensions that the spectral reflectances span [6].
- The ranking of the sensor-set color reproduction quality is mostly stable and not greatly affected by object categories [6].

These facts had been known from the experience, but

Table 1 Total number of collected spectral data for SOCS.

Category	No. of sub-categories	No. of colors
Photographic materials (Transparencies / Reflection prints):	8	2,304
Graphic printing (Offset / Gravure)	33	30,624
Color computer printers	21	7,856
Paint (for exterior / interior objects)		336
Paints (for art)	4	229
Textiles	6	2,832
Flowers		148
Leaves		92
Human skin		8,570
Krinov data (natural objects)		370
Total		53,361

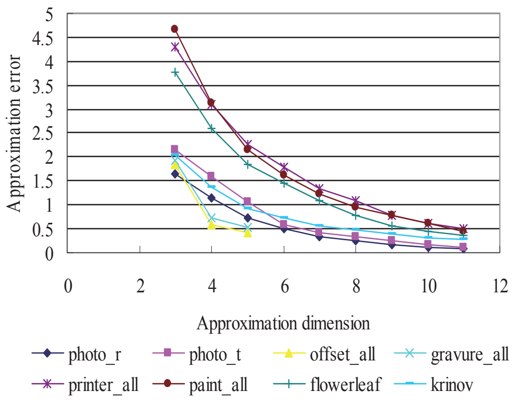

Fig.4 Approximation error using principal components for each category [4].

they were experimentally verified using SOCS. They are true under the daylight. However, it should be noted that the color appearance under the artificial illumination with many spectral peaks, like fluorescent lamps or LEDs, often differs from the one under the daylight. For example, it is known that fruit color looks as if it tastes better under the fluorescent lamps with three spectral peaks. However, the fruit in the image looks

(a) Color appearance under D65.

(b) Color appearance simulation under a fluorescent lamp.
Fig.5 Color appearance variation under various illuminations.

also good, when we restore the spectral reflectance from the image color using the three principal components of photographic materials (transparencies) in SOCS (Fig.5) and simulate its color. This means that, for example, oranges do not have any pigment that is unique to oranges. Such evaluation has become very important in the modern life, where various artificial illumination can be designed.

SOCS, which contains ca. 50,000 spectral data, is very useful for many applications. However, it may not be sufficient if it is regarded to contain all spectral reflectances/transmittances in the world: though it contains the data for flowers and leaves, it does not contain those for animals and fruits; the collection of inkjet printer inks is not enough either, since the inkjet technology has been greatly developed after the SOCS project. Another important category that was not included is that of fluorescent materials, which are constituents of papers and printer inks. Though it was considered, in the end it was not included in the database because the fluorescent materials are unstable and it was necessary to develop a new measurement method for the purpose. We hope that the database is continually developed and contributes to the new image sensing technology.

3. Computational color constancy and 'corresponding color reproduction'

Color constancy refers to the human visual function with which the human being can perceive the object color as almost stable under varying illumination. Computational color constancy is the machine vision algorithm to imitate this human physiological or psychological function. At first, it aimed at simultaneously computing both the spectral intensity of the illumination and the spectral reflectance of the object [7]. However, this problem turned out to be computationally unsolvable. Even the easier goal of estimating the illumination chromaticity from an image has not been achieved, either. It is now considered that, just as the human vision uses multiple cues to sense the distance from a scene, it utilizes diverse information in addition to the simple physical measurement at retina to estimate the object color, depending on the scene circumstances.

In the computational color constancy, many methods based on various cues have been proposed. For instance, we proposed a physics-based algorithm that uses the dichromatic reflection model [8]. When we aim at utilizing the obtained illumination chromaticity for 'Corresponding Color Reproduction,' which reproduces the scene colors that we perceive under different illuminations, another psychological approach should be combined.

It is known that the color of reflection light on a homogeneous surface of an non-metallic object can be modeled as Eq.(4): a linear combination of a diffuse reflection (the first term) and a specular reflection (the second term) with mixing coefficients α and β, where (R_o, G_o, B_o) is the object color and (R_w, G_w, B_w) is the illumination color. This model is called the "dichromatic reflection model [9]."

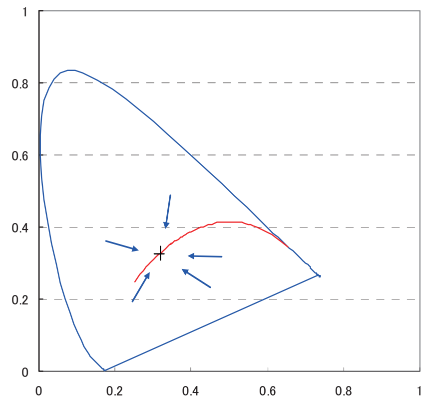

Fig.6. Chromaticity of dichromatically reflected light lies on straight lines (arrows) that cross at the chromaticity of the illumination (cross)..

$$\begin{pmatrix} R \\ G \\ B \end{pmatrix} = \alpha \begin{pmatrix} R_o \\ G_o \\ B_o \end{pmatrix} + \beta \begin{pmatrix} R_w \\ G_w \\ B_w \end{pmatrix} \tag{4}$$

If we consider the RGB three-dimensional space, the colors represented by this equation are distributed on a plane. If there are two object surfaces with different colors, their colors in a scene are distributed on two planes, which cross each other on a line. The line then represents the illumination color. If we show the relationship on a chromaticity diagram, a plane is replaced by a line, and a crossing point of two lines represents the chromaticity of the illumination (Fig.6). Hence, if there are multiple objects with different surface colors, the illumination chromaticity can be estimated as the nearest point from the multiple lines. If we express each line as Eq.(5), this problem can be formalized as that of minimizing $F(x,y)$ in Eq.(6), where w_i is the weight for each line.

$$a_i x + b_i y + c_i = 0 \tag{5}$$

$$F(x, y) = \sum_i w_i \frac{(a_i x + b_i y + c_i)^2}{a_i^2 + b_i^2} \tag{6}$$

Figure 7(b) shows the chromaticities of plastic objects in a scene (Fig.7(a)) measured by a spectroradiometer. It can be seen that the chromaticities (white dots) of plastic spoons are distributed on lines (each corresponding to the color of a spoon) that cross at a point, which corresponds to the chromaticity of the illumination, in this case white. It is known that this relation holds for most non-metallic objects [10].

In applying this principle to the automatic illumination chromaticity estimation, there remain several problems.

- The surface color of an object is not always homogeneous.
- Each colored object must be segmented in advance.

Though the color homogeneity holds in most artifacts, it does not hold in natural objects like flowers or leaves. Though it is hard to discriminate between artifacts and natural objects, we have developed an algorithm for the purpose with more than 80% accuracy [11]. The algorithm makes use of the property that most artifacts have long linear edges. This algorithm may be adopted to solve this homogeneity problem.

The segmentation problem will be solved by improving the 'color quantization' technique. Color

(a) A scene with plastic objects.

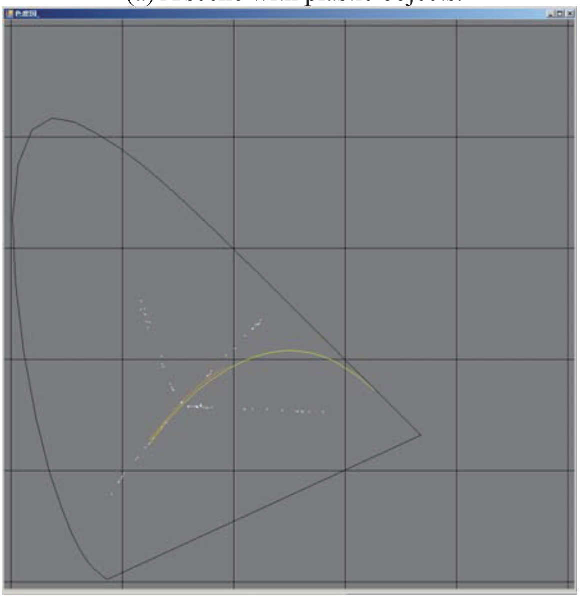

(b) Chromaticity diagram.

Fig.7 Chromaticity points of colors sampled from spoons.

quantization is a technique to express a full-color image with 8-bit RGB components by, e.g., less than 256 colors, by extracting dominant colors in the image. The technique was originally developed to save image memory [12]. For example, the full-color image in Fig.8(a) can be expressed by 33 colors as Fig.8(b), using this technique. To use this technique for illumination estimation, the number of colors can be reduced further, segmenting the image into connected color regions. Then the color distribution of each segment can be analyzed. One problem with this technique is that a color gradation due to shading can cause an over-division of regions with homogeneous colors. Improving the color quantization algorithm is also an important step for this illumination estimation.

Is it then possible to estimate the illumination chromaticity, if the segmentation problem is solved? Figure 9(a) is a raw image taken by a single-lens reflex camera under the illuminant A. Figure 9(b) is the result of illumination chromaticity estimation for the image, based on the five connected regions, i.e., the red, blue, green, yellow, and pink spoons, and a white color standard. Segmentation was manually carried out in this case. The white lines are the first principal components of the chromaticity distributions of the connected regions. Weighting the components with the number of the pixels in the regions, the point nearest to the lines (the red

(a) Original full color image with 24 bits/pixel.

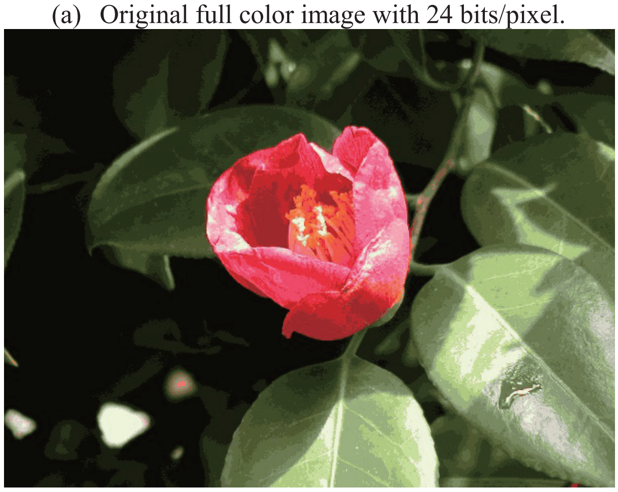

(b) The image expressed with 33 colors.

Fig.8 Color quantization

cross) was determined as the illumination chromaticity. Though it is estimated near the chromaticity of the standard white, the lines are not particularly well fitted to the chromaticity distribution. The distribution for the yellow region especially deviates from a line, forming a curve instead. Since the raw data were directly obtained from the color sensors, not mixed with the outputs from other channels, the reason for the curved distribution appears to be the non-linear characteristics of the sensor response. If we correctly calibrate the sensor response, the chromaticity distribution should fall on straight lines which should intersect at the illumination chromaticity. Hence, it is expected that correcting the non-linearity would simultaneously calibrate the sensors and estimate the illumination chromaticity.

We hypothesized that the non-linearity of the sensors is due to the S-shaped compensation, which is often applied in the photography industry. To remove the compensation, we modelled the S-shape characteristic by a hyperbolic function and tried a correction with its inverse function, allowing arbitrary shift (Eq.(7)).

$$y = \frac{1}{2} + \beta + \frac{1}{4\alpha}\log\frac{\rho - 1 + 2x - 2\delta}{\rho + 1 - 2x + 2\delta} \qquad (7)$$

Where α and ρ are constants that control the curvature of the S-shaped curve, and β and δ are those that control the shift. When we put a constraint that the curve passes two points $(x, y) = (0, 0)$ and $(1, 1)$, the curve shape is specified by two parameters, e.g. ρ and δ.

Figure 10 shows the result of such an optimization of

(a) An image taken under an illuminant A simulator.

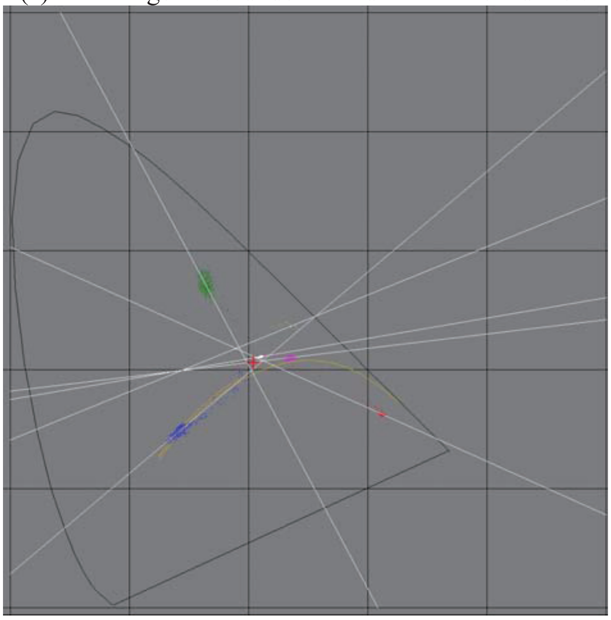

(b) Chromaticity distribution of the image.

Fig.9 Illumination chromaticity estimation using an existing single-lens reflex camera.

ρ and δ. Now the principal axis lines converge almost at a point near the chromaticity of the white standard. This effort to correct the response curve is not complete yet. Though the result for this camera looks good, the estimation accuracy is still not sufficient. Also, the method works worse for other cameras. More sophisticated optimization algorithm that can correct complicated curves may be necessary.

4. The relationship between color difference and genetic polymorphism

As the final topic, we introduce the color image processing from the biological viewpoint. This study is considered to be the first to investigate the relationship between the difference in perceived color and the genetic polymorphism among the normal color vision people.

Observers with normal color vision are trichromatic, and have three types of cones (L, M and S) on the retina. They are often treated as though they all have the same color perception property. However, it is known that the cone characteristics of normal trichromatic observers are not necessarily the same due to genetic polymorphism. This fact was not known when the CIE-1931 XYZ system was standardized.

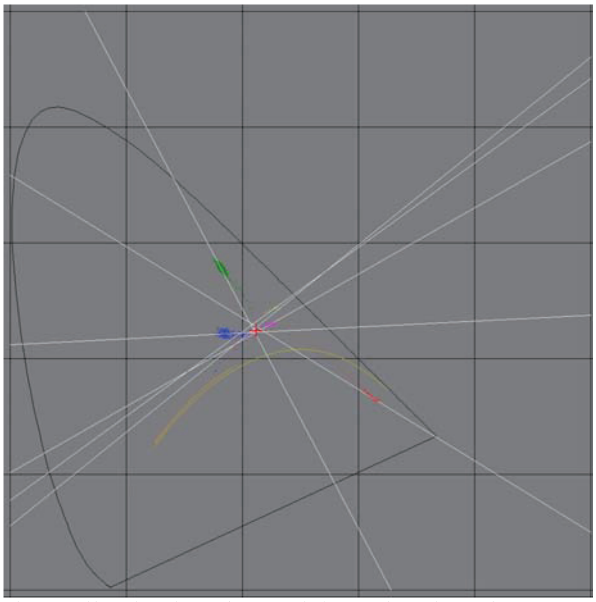

Fig.10 Illumination chromaticity estimation after sensor response correction.

The opsins, the light sensitive pigments, of the L and M cones are said to be the result of differentiation from one type, and very similar. One opsin has 364 amino acid residues, and 15 of them are different between L and M. Most of the spectral sensitivity difference between them is realized by the difference in 180th, 277th, and 285th amino acid residues [13]. The 180th amino acid residue is normally serine for an L opsin and alanine for an M opsin. However, it is often replaced by alanine even for an L opsin, and the absorption spectra analysis revealed that the spectral sensitivity of the L cone shifts to the short wavelength direction by 6nm [14]. We investigated how the wavelength shift relates to the color discrimination, and obtained an interesting result [15].

We postulated that, even if the L cone spectral sensitivity is shifted for a normal tri-chromatic observer, the neural or information processing that follows in the brain remains the same. Figure 11 (solid curves) shows the L, M and S spectral sensitivities $\bar{l}(\lambda)$, $\bar{m}(\lambda)$ and $\bar{s}(\lambda)$, which Hunt-Pointer-Estevez proposed, and $\bar{l}'(\lambda)$, which was obtained by shifting $\bar{l}(\lambda)$ by 6nm to the $\bar{m}(\lambda)$ direction. We call a person with $\bar{l}(\lambda)$, $\bar{m}(\lambda)$ and $\bar{s}(\lambda)$ 'a normal observer', and one with $\bar{l}'(\lambda)$, $\bar{m}(\lambda)$ and $\bar{s}(\lambda)$ 'a shift observer'.

Given these cone sensitivities and a light spectral in-

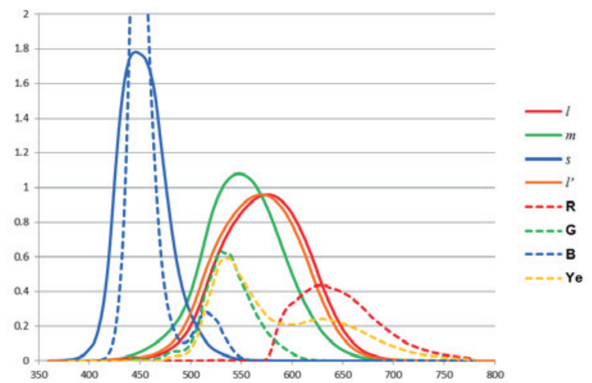

Fig. 11 Cone sensitivities (solid lines) with the shifted L cone sensitivity $\bar{l}'(\lambda)$, and primary colors' spectral intensity (dotted lines) of Quattron.

Table 2. The mean of measured L^*, a^* and b^* values of the first color of the color pairs, and the mean and the standard deviation of the measured color difference ΔE_{ab} between the first and second colors in the color pairs.

		Gray	Sky Blue 1	Yellow	Yellow Green	Skin	Sky Blue 2
L^*(Std)	Mean	75.259	76.825	71.527	77.512	74.351	76.752
a^*(Std)	Mean	1.842	9.057	–35.309	–49.868	–13.416	9.186
b^*(Std)	Mean	–10.762	–24.881	54.502	62.889	37.819	–24.993
ΔE_{ab}(Std)	Mean	1.042	1.066	0.742	1.079	0.260	0.418
	Std Dev	0.036	0.040	0.045	0.041	0.019	0.034
L^*(Shft)	Mean	75.365	77.041	71.547	77.648	74.207	76.965
a^*(Shft)	Mean	3.608	12.294	–33.640	–44.898	–15.766	12.365
b^*(Shft)	Mean	–10.578	–24.509	54.537	63.124	37.590	–24.626
ΔE_{ab} (Shft)	Mean	0.697	0.647	0.372	0.629	0.255	0.412
	Std Dev	0.030	0.031	0.033	0.029	0.015	0.031

tensity, we can calculate the tristimulus values L, M, and S. From them, CIE-1931 X, Y, and Z values, and CIE L^*, a^*, and b^* values can also be calculated. If we have a pair of lights or spectral intensities $\mathbf{P}_1$ and $\mathbf{P}_2$, we can also compute the color difference as the Euclidean distance between the two sets of L^*, a^* and b^* values. This is the procedure for the normal observer.

Likewise, we can calculate the color difference for the shift observer. In this case, as the L cone sensitivity is shifted, the output is L' instead of L, but the procedure that follows is the same. The color difference that the shift observer perceives should not be the same as the one the normal observer perceives.

To enhance the difference of the color difference, we used the four-primary-color display system Quattron by SHARP Corporation [16]. The Quattron has the primary Ye(llow) in addition to the normal primaries R, G, and B. The spectral intensities of the four primaries are depicted in Fig.11 with dotted lines.

The four-primary-color display Quattron can show a tri-chromatic observer various metamers of one color. However, because the metamers of one color for the normal observer are different from those for the shift observer, we can enhance the color difference between a color pair only for one of them and not for the other. Table 2 shows a set of six color pairs used in the experiment. For example, the first color of the 'Yellow' pair was (L^*, a^*, b^*)=(71.527, -35.309, 54.502) for the standard observer. The color difference ΔE_{ab} between the first and second color was measured several times, and the average and the standard deviation was 0.742 and 0.045, respectively. However, the first color was (L^*, a^*, b^*)=(71.547, -33.640, 54.537) for the shift observer. The average and the standard deviation of the color difference was 0.372 and 0.033, respectively. We used color pairs whose color difference is in the a^* direction, since the metamers generated by the Quattron for an observer have color differences in that direction for another observer.

In the subjective evaluation experiment, these color pairs were shown at upper and lower sides with separating horizontal black line on the Quattron display. The subjects (10 males with normal color vision) were asked which half looked redder. The pattern with the same pair with the inversed position was also prepared. The observation was repeated three times for verification.

The DNA sequences coding the amino acid residues of both L and M opsins of the subjects were determined with the nested PCR and the sequence analyzer. Genomic DNAs were prepared from saliva. The 180th, 277th, and 285th amino acid residues for each subject were determined. Table 3 shows the result of the above subjective evaluation experiment and the genetic analysis. The upper six rows show whether the subject could discriminate the color difference of each color pair. 'Yes' means that the subject could do it, and 'No' means that he could not. The next row shows the number of color pairs that the subject could discriminate. The 180th (the most important) amino acid residue of L opsin of the subject is shown. 'Ser' means serine, and 'Ala' means alanine. For example, the first subject could discriminate the color difference of four color pairs (Gray, Sky Blue 1, Yellow and Yellow Green), and his 180th amino acid residue of the L cone was alanine.

The experimental result was very interesting. Figure 12 shows the relationship between the number of subjects and the number of discriminable color pairs (NDCP). The subjects are classified with color according to the 180th amino acid residue of the L opsin. Except for one subject, the subjects who have alanine at that position discriminated more color pairs than those with serine. However, as we showed in Table 2, all color pairs were designed to have larger color difference for standard observers, who have serine at that position.

Table 3 The result of the observation experiment and the DNA analysis.

Subject No.	1	2	3	4	6	7	9	10	11	12
Gray	Yes	Yes	Yes	Yes	Yes	Yes	Yes	Yes	No	Yes
Sky Blue 1	Yes	Yes	Yes	Yes	Yes	Yes	Yes	No	Yes	Yes
Yellow	Yes	Yes	No	Yes	No	Yes	Yes	No	No	No
Yellow Green	Yes	No	No	Yes	No	Yes	Yes	No	No	No
Skin	No	No	No	No	No	No	No	No	No	No
Sky Blue 2	No	No	No	No	No	No	No	No	No	No
Number of Discriminable Color Pairs (NDCP)	4	3	2	4	2	4	4	1	1	2
L cone opsin 180th amino acid residue	Ala	Ala	Ser	Ala	Ser	Ser	Ala	Ser	Ser	Ser

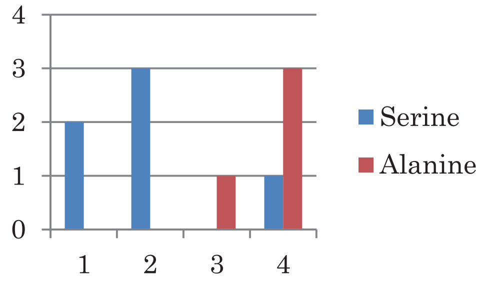

Fig. 12 The relation between NDCP and the 180th amino acid residue of the L cone opsin

We postulated that, even if the L cone spectral sensitivity on the retina is shifted, the neural or information processing that follows in the brain remains the same. The result of this experiment seems to show that the postulate was wrong. If the information processing is the same, the alanine at the 180th position should be a disadvantage for color discrimination. The result probably means that the individuals who were born with alanine at that position have grown up to have such information processing means that they discriminate colors better than those born with serine.

This experimental study is the first to investigate the relationship between color difference perception and genetic polymorphism. Since the experimental result was very interesting, more study should follow in many aspects. The number of subjects should be increased. The color difference evaluation in more directions than only in the *a** direction should be carried out. As the usable color difference direction was restricted by the characteristics of the Quattron, more sophisticated apparatus should be employed.

Only male subjects were used since the genes for L and M opsins are both on the X chromosome and the genetic analysis for females with their two X chromosomes is complicated. However, the experimental result was very interesting from the developmental viewpoint. It may be useful to deepen such studies for solving the problems in human vision, e.g., how the vision system grows up or how the color appearance in females is different from that of males, etc.

It is hoped that the understanding in color perception will be deepened by the collaboration of the image processing researchers with the biologists or biochemists.

5. Conclusions

Color images are often regarded only as a set of three gray images in the machine vision research community. Many research papers process RGB images without paying attention to the specification of the used RGB system. Such easy approaches may be allowable in some applications, but not in others. In applications that should be closely combined with the human vision, the viewpoints of biology and psychology should be taken into account.

In this paper, we introduced our researches from several viewpoints: the development of the basic database SOCS as well as a few unsolved problems. We expect the color image processing to be studied by many researchers in more serious manner, fusing various viewpoints.

Acknowledgement

This work was partially supported by KAKENHI 23500223.

References

[1] J. Tajima: Principles of Color Image Reproduction, Maruzen (1996) (in Japanese)
[2] H. E. J. Neugebauer: Quality Factor for Filters whose Spectral Transmittances are Different from Color Mixture Curves, and its Application to Color Photography. J. Opt. Soc. Am. Vol.46, No.10, 821-824 (1956)
[3] M. R. Pointer: The Gamut of Real Surface Colours, COLOR research and application, Vol.5, No.3, pp.145-155 (1980)
[4] J. Tajima, H. Haneishi, N. Ojima and M. Tsukada: Representative Data Selection for Standard Object Colour Spectra Database (SOCS). 10th CIC, 155-160 (2002)
[5] J. Tajima: A Huge Spectral Characteristics Database and its Application to Color Imaging Device Design, 6th CIC, 86-89 (1998)
[6] J. Tajima: Consideration and Experiments on Object Spectral Reflectance for Color Sensor Evaluation/Calibration. ICPR2000, 592-595 (2000)
[7] L. T. Maloney and B. A. Wandell: Color constancy: a method for recovering surface spectral reflectance. J. Opt. Soc. Am. A, Vol.3, No.1, 29-33 (1986)
[8] J. Tajima: Illumination Chromaticity EstimationBased on Dichromatic Reflection Modeland Imperfect Segmentation. Lecture Notes in Computer Science, Vol.5646, 51-61 (2009)
[9] S. A. Shafer: Using Color to Separate Reflection Components. Color Res. Appl., Vol.10, 210-218 (1985)
[10] S. Tominaga: Surface Identification Using the Dichromatic Reflection Model. IEEE Trans. PAMI-13, 658-670 (1991)
[11] J. Tajima, H. Kono: Natural Object/Artifact Image Classification Based on Line Features. IEICE Trans., Vol.E91-D, No.8, 2207-2211
[12] J. Tajima, T. Ikeda: High Quality Color Image Quantization. J. IIEEJ, Vol.18, No.5, 293-301 (1989) (in Japanese)
[13] J. Nathans, D. Thomas and D. S. Hogness.: Molecular genetics of human color vision: the genes encoding blue, green and red pigment. Science 232, 193-202 (1986)
[14] A. B. Asenjo, J. Rim and D. D. Oprian: Molecular determinants of human red/green color discrimination. Neuron 12, 1131-1138 (1994)
[15] J. Tajima, G. Tanaka, M. Suzuki, A. Moriyama and Y. Yoshida: Experiment on the Relation between Color Discriminability and Genetic Polymorphism in the L Cone Using Four Color Primary Display Device. 21st CIC, 180-184 (2013)
[16] K. Yoshiyama, H. Furukawa, N. Kondo, S. Nakagawa and Y. Yoshida: A new advantage of multi-primary-color displays. SID Symposium Digest of Technical Papers, 281-282 (2010)